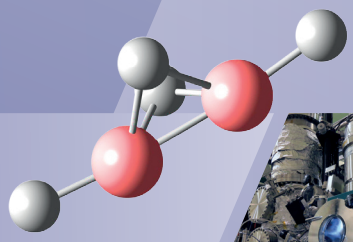

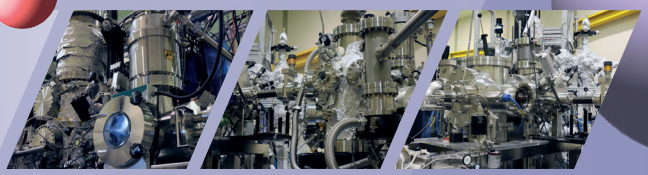

Molecular Science

Defeating Air Pollution: Unraveling the Pathogenic Mechanism of PM2.5

Aerosols, referring broadly to ultrafine particulate matter (PM) suspended in a gaseous medium, are found to play increasingly important roles in atmospheric chemistry, environmental science, public health and biomedical sciences in the past five years; see Fig. 1 for correlations of aerosol science with various associated research fields.

Although naturally produced aerosols are essential to maintain the radiative balance for Earth, anthropogenic aerosols produced from various human activities, such as industrial processes, transport emissions and coal burning have severely disturbed the homeostasis of Earth's environment. These unnaturally produced aerosols have altered the microphysics of the formation and growth of clouds, altered atmospheric photochemical processes, worsened air quality and caused marked adverse health effects for human beings. As reported by the International Agency for Research on Cancer of the World Health Organization (WHO), exposure to ambient fine PM in polluted air contributed to 3.2 million premature deaths worldwide in 2010; amongst them 223,000 mortalities were due to lung cancers.[1] In an updated WHO report released in 2014, the mortalities associated with exposure to air pollution increased to 7 million in 2012, accounting for 1/8 of total global deaths. These findings stress unambiguously the facts that air pollution and the PM suspended therein have become the largest environmental factor contributing to human health risk and mortality. Among all PM suspended in the air, PM2.5, which is defined as PM with an aerodynamic diameter smaller than 2.5 μm, are particularly harmful to human bodies. While large PM (> 2.5 μm), once inhaled might be removed by lung mucous and cilia, PM2.5 can penetrate to the alveolar, the deepest region of the lung in which occurs an exchange of gas between air and blood, or even enter the systemic circulation to cause further adverse health effects.

Even though the correlations between PM2.5 and various morbidities, including pulmonary and lung diseases, cardiovascular diseases and cancers, have been well established from epidemiology studies, their pathogenic mechanisms remain elusive at the molecular level. The reason is mainly that our understanding of the fundamental physical, chemical and biological properties of PM2.5 as well as of the biomolecules that are vulnerable to attack by PM2.5, is insufficient. Among varied intrinsic characteristics, the valence-electronic structure and ionization energy of a substance are especially crucial as these properties decisively determine the chemical activities of the substance with other chemical species. Whereas the valence electronic properties of PM2.5 might depend critically on the size, shape, composition and internal architecture, the valence-electronic properties of a biomolecule might also rely crucially on the aqueous environment in which they reside and conduct their biological functions, through the pronounced solvent-solute interaction and hydrogen-bond effect.

With the objective to understand the valence- electronic properties of both PM2.5 and the biomolecules that are likely vulnerable to be affected by PM2.5, and eventually to clarify the pathogenic mechanism of PM2.5 in leading to various morbidities, a research team led by Chia C. Wang of National Sun Yat-Sen University has recently developed a novel apparatus to record the VUV photoelectron spectra of aerosols; this spectrometer is capable of measuring the valence-electronic structural properties of both PM2.5 and solvated biological molecules, as shown in Fig. 2.[2] The VUV radiation generated via undulator U9, at **BL21B2**, served as the ionization source. The usage of VUV plays a determining role in the experiments on photoelectron spectra of aerosols as it provides a soft mechanism for ionization, allowing the valence-level electronic structures of target aerosol species and their electronic evolutions to be measured, rather than the core-level electrons typically measured in X-ray photoelectron spectra.

In this featured work, Wang and her research team have chosen a unique and biologically important amino acid, cysteine (Cys), to study its valence-electronic properties and the evolution in its aqueous aerosol form, and in so doing to demonstrate the strength of the newly constructed apparatus. Through the active thiol (-SH) group at its side chain, Cys is highly nucleophilic and generally plays a key role in many important redox-based biological processes, including mediating the signaling paths and regulating the activi-

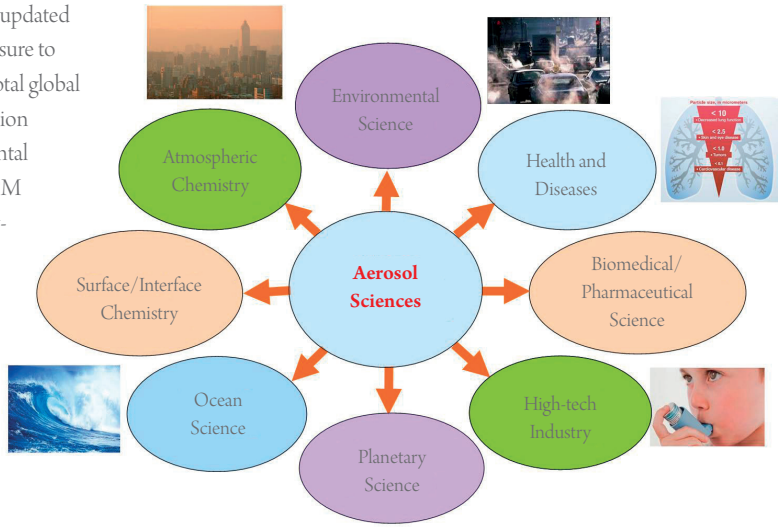

Fig. 1: Illustration of the correlations of aerosol science with several important fields.

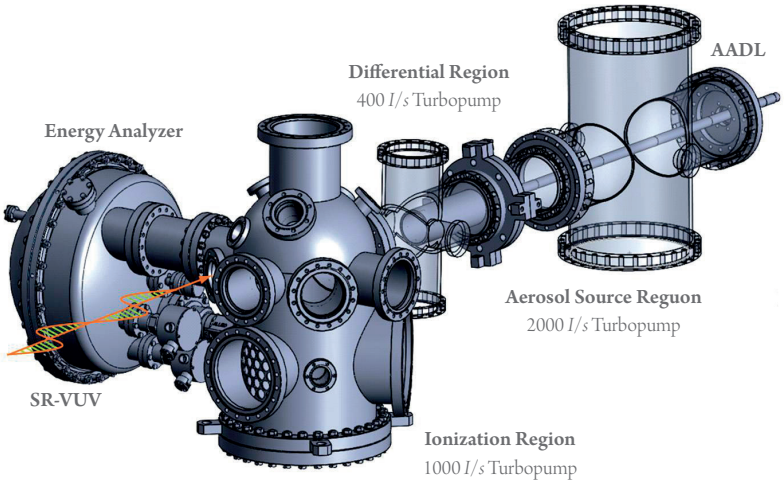

Fig. 2: Schematic view of the aerosol VUV photoelectron spectroscopy apparatus. The polarization vector of SR-VUV (**BL21B2**) is specified. [Reproduced from Ref. 2]

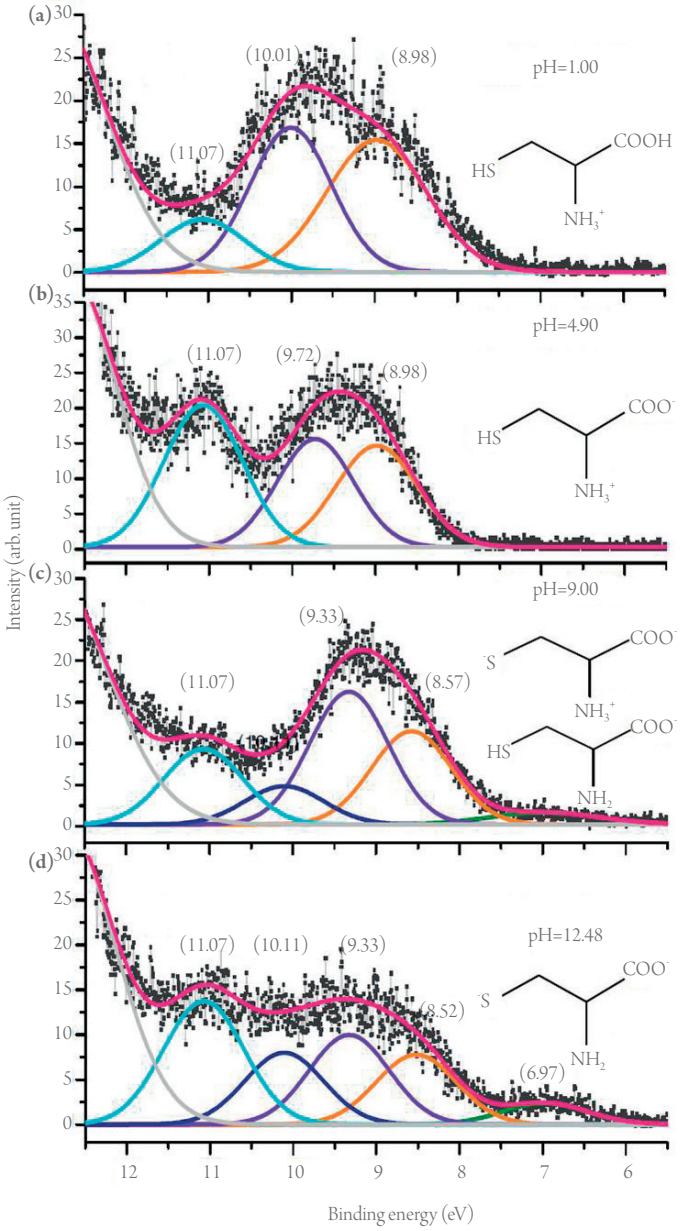

Fig. 3: VUV photoelectron spectra of Cys aqueous aerosols at four chosen pH conditions measured at 25 eV. A. pH =1.00, B. pH = 4.90, C. pH = 9.00 and D. pH = 12.48. Symbols: experiment, -▪-; Cys n_s', green curve; Cys n_s, orange curve; Cys n_O, violet curve; Cys n_N, blue curve; condensed water, cyan curve; gaseus water (only partial), grey curve; cumulative curve, pink curve. [Reproduced from Ref. 2]

ties of enzymes via S-nitrosylation and thiol oxidation. Despite the biological significance, the valence electronic properties of Cys in aqueous environments were unavailable before this work.

In this featured work, Cys was introduced into the aqueous aerosol phase of size ~ 100 nm, which readily created a bulk aqueous environment on a nanometre scale, allowing the valence-electronic properties of Cys and its possible evolution with altering aqueous environments to be studied in a systematically controlled way. Because Cys exhibits three possible sites of deprotonation, these varied forms of protonation and deprotonation are dominant at varied pH values. To learn how the valence-electronic properties of Cys are affected by the altering local chemical environments or by the varying nature of its charged status, Prof. Wang and coworkers measured VUV photoelectron spectra of Cys aqueous aerosols at selected values pH = 1.00 (Fig. 3(a)), 4.90 (Fig. 3(b)), 9.00 (Fig. 3(c)) and 12.48 (Fig. 3(d)) at 25 eV, with each pH condition representing a major chemical species. The photoelectron spectra of Cys aqueous aerosols in the four aqueous conditions explicitly show distinct photoelectron band shapes, reflecting the modified molecular-orbital character of Cys as the local chemical environment varies with pH. The ionization energy of Cys in an aqueous solution of small pH has been determined for the first time to be 8.98 ± 0.05 eV. It is notable that a new spectral feature was observed at pH = 9.00 and 12.48 with a smaller binding energy, 6.97 ± 0.05 eV, indicating that the negative charge on the thiolate group becomes the first electron to be removed upon ionization. The results reported in this featured work provided a new microscopic perspective to understand the nucleophilicity of Cys at varied pH. The authors showed that Cys loses an electron more easily with increasing pH, and a new ionization channel with a smaller energy barrier becomes open when the thiol group is deprotonated. As outlined in Marcus's charge-transfer (CT) theory, this result implies that, when Cys is involved in a redox process, the CT path might be entirely altered when its local chemical environment varies with pH, and accordingly the rate and efficiency of CT. The results illustrated in this work consequently provide valuable hints to enable one to understand how the biochemical activity of Cys becomes affected when the active and oxidizing components of PM2.5 interact with the highly nucleophilic Cys upon inhalation. From a more general perspective, this featured work provides an elegant example to demonstrate how sensitively the valence-electronic properties of an aerosol can be affected by its local chemical environment.

This novel VUV aerosol technique presents valuable and promising opportunities to study fundamental and important properties of both aerosols and solvated biological molecules in an aqueous aerosol form, and to address critical issues regarding PM2.5 and its related fields, including environmental science, atmospheric chemistry and biomedical science. We remark additionally that the authors in this featured work demonstrated elegantly also the power of using of the new approach to record photoelectron spectra of an aqueous aerosol so as to probe solvated species, and its advantages over the conventional liquid microjet technique. By overcoming the electrokinetic charging issue that is typically encountered in the liquid microjet technique and by considerably improving the spectral resolution, detailed insight regarding the solvated species and the aerosols can be expected to be unraveled via this newly developed approach. In the near future, Wang and her research team are planning to investigate more environmentally important PM2.5, with a focus on clarifying the fundamental mechanisms underlying the adverse impacts of PM2.5 on human health at a molecular level. (Reported by Yin-Yu Lee and Chia-Chen Wang)

This report features the work of Chia-Chen Wang and her co-workers published in J. Phys. Chem. Lett. ***6****, 817 (2015).*

References

1. S. C. Anenberg, L. W. Horowitz, D. Q. Tong, and J. J. West, Environ. Health Perspect. **118**, 1189 (2010).
2. C.-C. Su, Y. Yu, P.-C. Chang, Y.-W. Chen, I. Y. Chen, Y.-Y. Lee, and C. C. Wang, J. Phy. Chem. Lett. **6**, 817 (2015).

Synthesis of a New Structure B_2H_4 from B_2H_6

Diborane molecules are composed of two boron atomic centers and multiple hydrogen atoms, hence represented as B_2H_x. The structures of diborane species are still controversial. The normally existing B_2H_6 contains two bridging B-H-B bonds and four terminal B-H bonds in the calculated most stable conformation; gaseous samples show also a central B-B bond. Other B_2H_x might be synthesized in collisions of H_2 and boron atoms but no neutral diboron hydride species with less than six H atoms and a bridging B-H-B bond has been experimentally observed.

Bing-Ming Cheng and his co-workers dispersed B_2H_6 in neon on a KBr window at 3 K. They utilized the advantages of synchrotron radiation at **BL21A2** to direct the vacuum-ultraviolet light onto the neon surface with wavelengths varied from 115 nm to 220 nm.[1] With excitation energies at light wavelengths 200 nm and 220 nm, a product was identified with infrared absorption spectra to be B_2H_2, previously detected elsewhere. On decreasing the wavelength of VUV light to 180 nm, many IR absorption features of other products appeared, as partly shown in Fig. 1. The structures observed by others failed to fit these new absorption signals, so diborane molecules of an entirely new structure should have been synthesized.

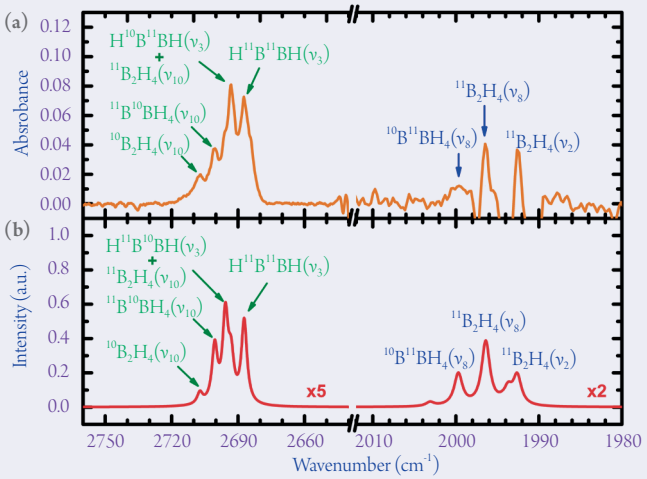

Fig. 1: Infrared absorption of B_2H_4 in modes ν_2, ν_8 and ν_{10}, (a) from photolysis of B_2H_6/Ne = 1/1000 at 3 K upon excitation at 122.6 nm and (b) from simulations. Some assignments are indicated.

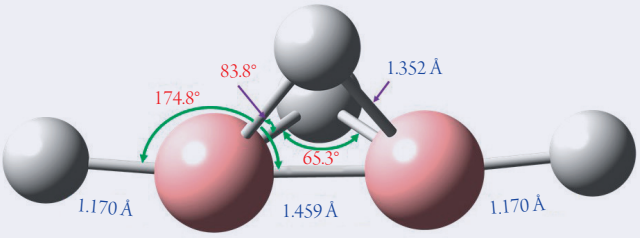

Fig. 2: Calculated structure of B_2H_4.

Cheng and his co-workers carefully undertook new quantum-chemical calculations of the harmonic and anharmonic vibrational motions to calculate the wavenumbers and intensities of each vibrational mode for various conformers. They eventually recognized the vibrational characteristics of neutral B_2H_4 with two bridging B-H-B bonds and two terminal B-H bonds that satisfactorily fit the newly observed absorption features of the synthesized diborane species. The calculated structure of B_2H_4 is shown in Fig. 2.

There are two major boron isotopes in nature, ^{11}B and ^{10}B; the boron atoms in B_2H_4 could hence be $^{10}B^{10}B$ or $^{10}B^{11}B$ or $^{11}B^{11}B$. As the atomic masses differ, the vibrational frequencies also vary. In Fig. 1, some vibrational modes for all $^{10}B^{10}BH_4$, $^{10}B^{11}BH_4$ and $^{11}B^{11}BH_4$ were observed. To confirm the structure of the new species, neutral B_2H_4, Cheng replaced the hydrogen atoms with deuterium atoms. Both the absorption spectra and the calculated vibrational energies of B_2D_4 conform to the calculated structure shown in Fig. 2. On that basis they assigned this new species as diborane(4). Because the infrared absorption features appear with vacuum-ultraviolet photons of wavelength 180 nm, the photolysis threshold to synthesize diborane(4) is about 6.6 eV. Although the detailed process of the dissociation and synthesis is still unrevealed, the new species is definitely formed from the precursor with vacuum-ultraviolet light as confirmed with infrared spectra. (Reported by Chen-Lin Liu)

This report features the work of Bing-Ming Cheng and his co-workers published in Chem. Sci. ***6****, 6872 (2015).*

Reference

1. S.-L. Chou, J.-I. Lo, Y.-C. Peng, M.-Y. Lin, H.-C. Lu, B.-M. Cheng, and J. F. Ogilvie, Chem. Sci. **6**, 6872 (2015).

Highly Selective Dissociation of Peptide Bonds

Molecules are composed of atoms and chemical bonds. To control a chemical reaction, breaking and forming specific chemical bonds is a key aspect. The use of photons to control the cleavage of a selected chemical bond in a complicated molecule remains a challenge in chemistry. Photochemists traditionally vary the ratios of cleavages of chemical bonds on tuning monochromatic radiation, typically in the ultraviolet region, to the energies of excited states of precursor molecules, but the selectivity is limited. This method has been extended on combining infrared and ultraviolet photons and using vibrationally mediated photodissociation to control further the breakage of a chemical bond for small polyatomic molecules. An optimally shaped, strong-field laser pulse provides another method to control the cleavage of a specific chemical bond; shaping the pulse is a complicated process that has so far been applied to only few molecules.

A third method utilizes the near-edge X-ray absorption of core electrons, in which the energy of a photon to excite a particular atom is sensitive to that atomic chemical environment. On tuning the X-ray wavelength to the K-edge absorption of atoms of a particular element, one might excite selectively that specific atomic entity. Such selective excitation can be specific to either an element or a site of the same element. An X-ray absorption corresponds to an excitation from the 1s orbital of this particular atom to an empty valence orbital or to direct ionization. One major channel after

excitation is Auger decay, an ejection of one or two electrons, followed by dissociation. If the excitation energy remains localized near an initially excited atom, the chemical bonds around the excited atom might break readily.[1] Element-selective or site-selective bond breaking following core-level excitation has been observed for molecules on a surface and in the gaseous phase, but the branching ratios (or selectivity) of these site-specific or bond-specific dissociation are typically small.

Chen-Lin Liu and his co-workers discerned the possibility to break specific chemical bonds via core excitation of a specific location of a molecule. They built at **BL05B1** a new end-station composed of an orthogonal acceleration reflectron time-of-flight mass spectrometer, matrix-assisted laser desorption and ionization, hemispherical energy analyser, etc. They observed some obviously enhanced products following specific core excitation for some aromatic molecules, such as phenol, but no intuitive relation between a location of excitation and breaking bonds was confirmed.[2] They thought that the reason might be that it is necessary to break two chemical bonds for the cyclic structure. They would apply the phenomenon of specific dissociation to bio-molecules for possible structural characterization. Two molecules, N-methylformamide and N-methylacetamide, were chosen as models of peptide molecules, as the OC–N bond has the same structure as the peptide bond in peptides connecting various amino acids.[3]

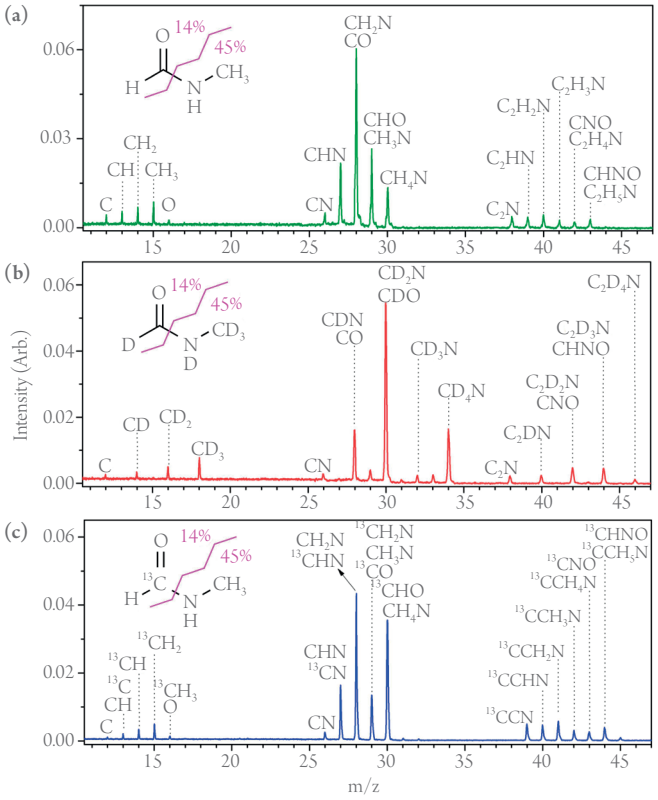

Fig. 1: Mass spectra of three isotopic species of N-methylformamide excited at C 1s → π*.[3]

Shown in Fig. 1(a) is the mass spectrum of N-methylformamide excited at the C K-edge. The ratio of mass to charge of the dominant products is 27 – 30 u. To distinguish whether they are products from a specific dissociation, their branching ratios were drawn as in Fig. 2. The products with m/z = 28 u have larger branching ratios following 1s → π* transitions at the C, N, and O K-edges. The branching ratio was enhanced from 20 % to 35 % at N and O K-edges, so confirming the product from a specific dissociation. Tracing the mechanisms of specific dissociation, they performed the same experiments for isotopically substituted molecules, producing the mass spectra shown in Figs. 1(b) and 1(c). The branching ratios of all dissociation channels of all products were also calculated clearly. The major compositions of each product are thus listed above the signals in Fig. 1. Furthermore, the major dissociation mechanism of the enhanced product with m/z = 28 u was found to be breakage of the OC–N bond with branching ratios as great as 59, 71 and 61 % at the C, N, and O K-edges, respectively. Liu undertook the same experiments with another peptide model, N-methylacetamide, with similar results, which confirmed this specific breaking of the peptide bond. Applying this phenomenon to peptides, the mass spectra will show ideally the compositions as easily as of amino acids. This condition might simplify the analysis and make structural identification more accurate. (Reported by Chen-Lin Liu)

This report features the work of Chen-Lin Liu and his co-workers published in J. Phys. Chem. A ***119****, 6195 (2015).*

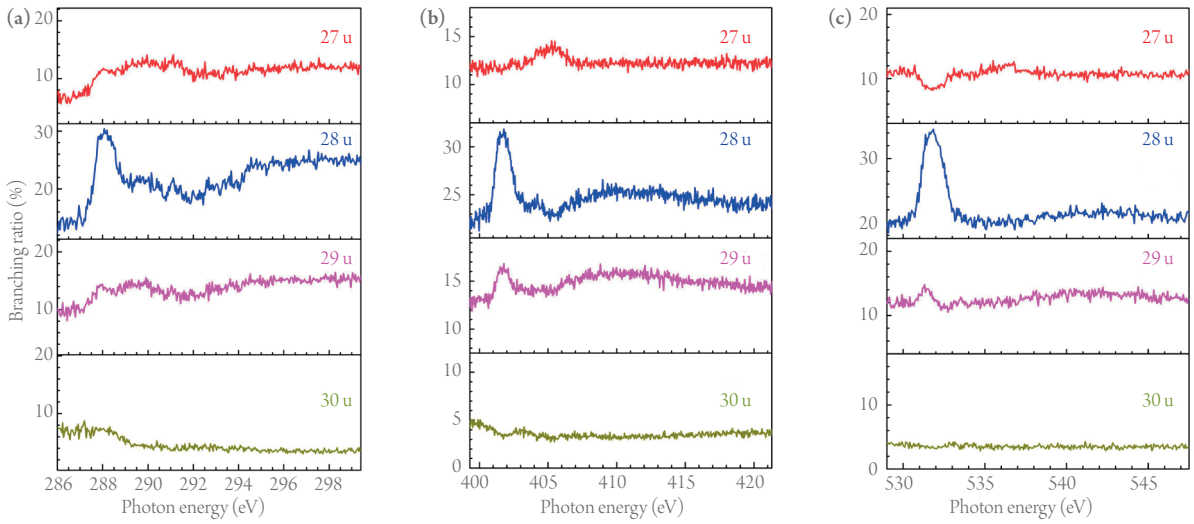

Fig. 2: Branching ratios of the dominant products of N-methylformamide following 1s → π* transitions at the (a) C K-edge, (b) N K-edge, and (c) O K-edge.[3]

References

1. W. Eberhardt, T. K. Sham, R. Carr, S. Krummacher, M. Strongin, S. L. Weng, and D. Wesner, Phys. Rev. Lett. **50**, 1038 (1983).
2. Y.-S. Lin, K.-T. Lu, Y. T. Lee, C.-M. Tseng, C.-K. Ni, and C.-L. Liu, J. Phys. Chem. A **118**, 1601 (2014).
3. Y.-S. Lin, C.-C. Tsai, H.-R. Lin, T.-L. Hsieh, J.-L. Chen, W.-P. Hu, C.-K. Ni, and C.-L. Liu, J. Phys. Chem. A **119**, 6195 (2015).